

Rock properties inversion with Kirchhoff AVA migration/inversion

Jiang Feng and M. D. Sacchi, University of Alberta, Edmonton, Canada

2004 CSEG National Convention



Abstract

This paper proposes a strategy to perform amplitude versus angle (AVA) and rock properties inversion simultaneously by applying conjugate gradient (CG) method on a ray-based Kirchhoff migration/inversion scheme in the angle domain. The idea is to use the Kirchhoff integral formulation to estimate rock physical parameters directly from pre-stack seismic data by using relationship between AVA and elastic parameters (i.e., Zoeppritz Equations). Implementation of the method shows successfully delineating subsurface structure and recovering local changes in the rock properties for a 2D model.

Introduction

Imaging using ray based Kirchhoff migration/inversion is a very common application in exploration geophysics (Keho and Beydoun, 1988; Gray and May, 1994; Akbar et al., 1996). Nowadays, the goal of the migration changes from imaging subsurface structure to recovering elastic properties (Beydoun and Mendes, 1989). As the rock parameters are not related linearly to the seismic reflection data (Lumley and Beydoun, 1997), the inversion for elastic constants must be performed in two steps:

- 1) The seismic data are transformed to common image gathers (CIG) by migration or inversion. This step requires a migration algorithm for complex media that preserves amplitudes.
- 2) Using approximations to the Zoeppritz equations (Aki and Richards, 1980; Shuey, 1985; Fatti et al., 1994) then, transform the CIGs to perturbations of the elastic parameters (Beretta et al., 2002; Li et al., 2003).

Our Imaging technique is mainly based on the work on Kirchhoff inversion algorithms developed by Bleistein (1987, 1997, 2002) and Xu (2001). In particular, we implement our algorithm as a least-squares migration problem where we estimate elastic parameter perturbations directly from pre-stack data.

Method

Let us begin with the linear scattering problem of the form

$$d = W L m + n_1, \quad (1)$$

where d denotes the seismic data, m refers to the Earth model (CIG), n_1 is the noise, W represents the wavelet, and L represents the Kirchhoff forward operator. In the frequency domain, the above equation can be written as

$$d(\mathbf{r}, \mathbf{s}, \omega) = i\omega \int m(\mathbf{x}, \theta) A(\mathbf{r}, \mathbf{x}, \mathbf{s}) [\bar{\mathbf{n}} \cdot \nabla \tau(\mathbf{r}, \mathbf{x}, \mathbf{s})] e^{i\omega\tau(\mathbf{r}, \mathbf{x}, \mathbf{s})} W(\omega) d^3 \mathbf{x} + n_1(\omega). \quad (2)$$

where \mathbf{s} denotes the source position, \mathbf{r} is the receiver position, ω refers to the angular frequency, θ refers to the reflection angle, the arbitrary space position \mathbf{x} is defined by (x_1, x_2, x_3) , $\bar{\mathbf{n}}$ represents the normal direction unit, A refers to the amplitude (geometrical-spreading factor from source \mathbf{s} to receiver \mathbf{r} via \mathbf{x}) and τ refers to the travelttime. Note that the CIGs m is to rock parameter via a Zoeppritz forward operator Z ,

$$m = Z p + n_2, \quad (3)$$

where modeling errors can be included in the term n_2 . For PP reflections, Aki and Richards provide the following operator

$$m(x, \theta) = \frac{1}{2} \left(1 - 4 \frac{v_s^2}{v_p^2} \sin^2(\theta) \right) \frac{\Delta \rho}{\rho} + \frac{\sec^2(\theta)}{2} \frac{\Delta v_p}{v_p} - 4 \frac{v_s^2}{v_p^2} \sin^2(\theta) \frac{\Delta v_s}{v_s} + n_2 \quad (4)$$

where ρ , v_p , v_s are the average of density, P-wave velocity and S-wave velocity of adjacent two layers. Furthermore, $\Delta \rho$, Δv_p , Δv_s are the differences of the density, P-wave velocity and S-wave velocity of two adjacent layers, respectively. The angle θ is the average of incidence and transmission angles. In the case of negligible difference of the elastic parameters, this angle θ can be approximated by the reflection angle. Combining equation (1) and (3), the seismic data can now be expressed by

$$d = WLZp + n \quad (5)$$

We then estimate p from d by minimizing the cost function J , which is the sum of a data space misfit and a model space function, basing on the assumption that the noise is Gaussian and uncorrelated

$$J = \|d - WLZp\|^2 + \alpha_1 \left\| \frac{\partial p}{\partial x_1} \right\|^2 + \alpha_2 \left\| \frac{\partial p}{\partial x_2} \right\|^2 + \beta |p|. \quad (6)$$

The last term is a l_1 model norm used to “spike” up the final solution. The solution to the cost function is

$$p = (Z^T L^T W^T WLZ + \alpha_1 Q_1^T Q_1 + \alpha_2 Q_2^T Q_2 + \beta Q^T Q)^{-1} Z^T L^T W^T d, \quad (7)$$

where τ means transpose (or adjoint/migration operator). Q_1 and Q_2 are the first order derivatives (smooth operators) in the equation (6) along x_1 and x_2 directions respectively. Q is the diagonal matrix defined as

$$Q_{ii} = \frac{1}{\sqrt{|p_i|}} \quad (8)$$

Generally, it is too expensive to calculate the inverse of the terms inside the brackets of the equation (7) (for example, inverting a matrix via direct solvers is an N^3 process for an $N \times N$ matrix). Therefore, we use CG to minimize cost function J . The cost can then be minimized in cost proportional to $K \times N^2$, where K is the number of iterations. For seismic inversion, it is always true that $K \ll N$; thus, this method is more efficient than a direct determination of the inverse operator.

The CG algorithm needs the forward and adjoint operators (for details see Scales, 1987). To derive these operators, we rewrite our optimization goal as a system of observations of the form

$$\begin{pmatrix} d \\ \mathbf{0} \end{pmatrix} = \begin{pmatrix} WLZ \\ \sqrt{\alpha_1} Q_1 \\ \sqrt{\alpha_2} Q_2 \\ \sqrt{\beta} Q \end{pmatrix} p \quad \text{Forward} \quad (9)$$

$$\hat{p} = \begin{pmatrix} Z^T L^T W^T & \sqrt{\alpha_1} Q_1^T & \sqrt{\alpha_2} Q_2^T & \sqrt{\beta} Q^T \end{pmatrix} \begin{pmatrix} d \\ \mathbf{0} \end{pmatrix} \quad \text{Adjoint} \quad (10)$$

where d , $\mathbf{0}$, p and \hat{p} can be vectors, matrices or multidimensional cubes.

Example

A 2D acoustic geological model was created to test accuracy of this approach (Figure 1A). The model has 7 layers, including a fold, a pinch out and interfaces with topography. The synthetic data sets (Table 1) were calculated for this model using Seismic Unix modelling program.

Table 1: Information of shot and receiver

Number of shots	Shot spacing [m]	First shot position [x, z] [m]	Number of receivers per shot	Receiver spacing [m]	First receiver's offset [m]
51	20	[2000, 0]	201	20	2000

The synthetic data sets were inverted for the rock properties (Figure 1B and 1C) using the method outlined above. The recovered structure of the layers is clear and correct. The common reflection angles gathering at $x = 3600$ meters (Figure 2A) shows coherent and continuous events for a wide range of reflection angle and alias cannot be seen. The picked AVA (Figure 2B) matches the theoretical values for large angle. The theoretical equation for AVA is given by

$$R(\theta_1) = \frac{\rho_2 v_2 \cos \theta_1 - \rho_1 v_1 \cos \theta_2}{\rho_2 v_2 \cos \theta_1 + \rho_1 v_1 \cos \theta_2} \quad (11)$$

where R is angle dependent reflectivity, ρ_1 , ρ_2 , v_1 , v_2 are densities and velocities of upper and lower layers respectively, θ_1 , θ_2 are the incident and transmitted angles respectively. The comparison between the inverted and true rock properties shows that the inverted rock properties match the true rock properties well (Figure 3). As no energy loss due to transmission is included in this algorithm, the accuracy of the inversion result degrades for lower horizons.

Conclusion

We have proposed the AVA and rock properties inversion algorithm. The main advantages are: 1) the structure of the subsurface is imaged well, even for complex structure, 2) events are continuous in common reflection gathers, and AVA responds in wide range of angles, 3) the algorithm does not depend on acquisition geometry, 4) rock properties are inverted directly in one step, 5) ray based Kirchhoff operator is efficient for target-oriented inversion. However, at current state the algorithm does not handle transmission losses thus debasing the inversion results for deeper reflectors. As exploration targets usually found at greater depth, future work will concentrate on enhancing the image of deep and complex interfaces.

Acknowledgements

The authors would like to thank EnCana, Geo-X Ltd, Veritas Geoservices, AERI - Department of Energy, Province of Alberta, and N.S.E.R.C. for funding this research. In addition, the authors thank Ulrich Theune and Yiqian Wang for their helpful suggestions and proofreading.

References

- Akbar, E. F., Sen, K. M., and Stoffa, L. P., 1996, Prestack plane-wave Kirchhoff migration in laterally varying media: *Geophysics*, **61**, 1086-1079.
- Aki, K., and Richards, P. G., 1980, *Quantitative Seismology: theory and methods*: Freeman, New York.
- Beretta, M., Bernasconi, G., and Drufuca, G., 2002, AVO and AVA inversion for fractured reservoir characterization: *Geophysics*, **67**, 300-306.
- Beydoun, W. B., and Mendes, M., 1989, Elastic ray-Born L_2 -migration/inversion: *Geophys. J.*, **97**, 151-160.
- Bleistein, N., 1987, On the imaging of reflectors in the earth: *Geophysics*, **52**, 931-942
- Bleistein, N., Cohen, J. K., and Stockwell, J. W., 2001, *Mathematics of Multidimensional Seismic Imaging, Migration, and Inversion*: Springer, New York.
- Bleistein, N., Gray, S. H., 2002a, From the Hagedoorn Imaging Technique to Kirchhoff Migration and Inversion: Center for Wave Phenomena, Colorado School of Mines.
- Bleistein, N., Gray, S. H., 2002b, A Proposal for Common-Opening-Angle Migration/Inversion: Center for Wave Phenomena, Colorado School of Mines.
- Downton, E. J., and Lines, R. L., 2002, AVO NMO: CSEG 2002 abstract.
- Downton, E. J., and Lines, R. L., 2003, High-resolution AVO NMO: CSEG 2003 abstract.
- Fatti, J. L., Smith, G. C., Vail, P. J., Strauss, P. J., and Levitt, P. R., 1994, Detection of gas in sandstone sandstone reservoirs using AVO analysis: A 3-D seismic case history using the Geostack technique: *Geophysics*, **59**, 1362-1376.
- Gray, H. S., and May, P. W., 1994, Kirchhoff Migration using Eikonal Equation Traveltimes: *Geophysics*, **59**, 810-817.

Keho, T. H., and Beydoun, W. B., 1988, Paraxial ray Kirchhoff migration: *Geophysics*, **53**, 1540-1546.

Li, Y. Y., Goodway, B., and Downton, J., 2003, Recent Advances in Application of AVO to Carbonate Reservoirs: *Recorder*, **28**, 34-40.

Lumley, D. E., and Beydoun, W. B., 1997, Elastic parameter estimation by Kirchhoff prestack depth migration/inversion: *SEP report*, **70**, 162-190.

Scale, J. A., 1987, Tomographic inversion via the conjugate gradient method: *Geophysics*, **52**, 179-185.

Shuey, T. R., 1985, A simplification of the Zoeppritz equations: *Geophysics*, **50**, 609-614.

Tarantola, A., 1987, *Inverse problem theory: Methods for data fitting and model parameter estimation*: Elsevier Science Publishing Company Inc.

Xu, S., Chauris, H., Lambare, G., and Noble, M., 1990, Common-angle migration: A strategy for imaging complex media: *Geophysics*, **66**, 1877-1894.

Youzwishen, C., 2001, *Non-linear sparse and blocky constraints for seismic inverse problems*: MS thesis, University of Alberta

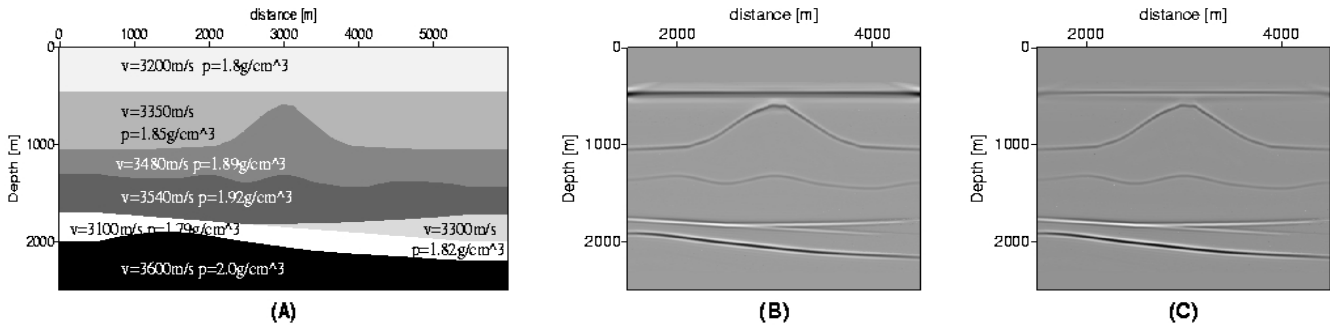


Figure 1: Acoustic geological model for the synthetic data sets (A). The corresponding inverted model for $\frac{\Delta v}{v}$ (B) and $\frac{\Delta \rho}{\rho}$ (C).

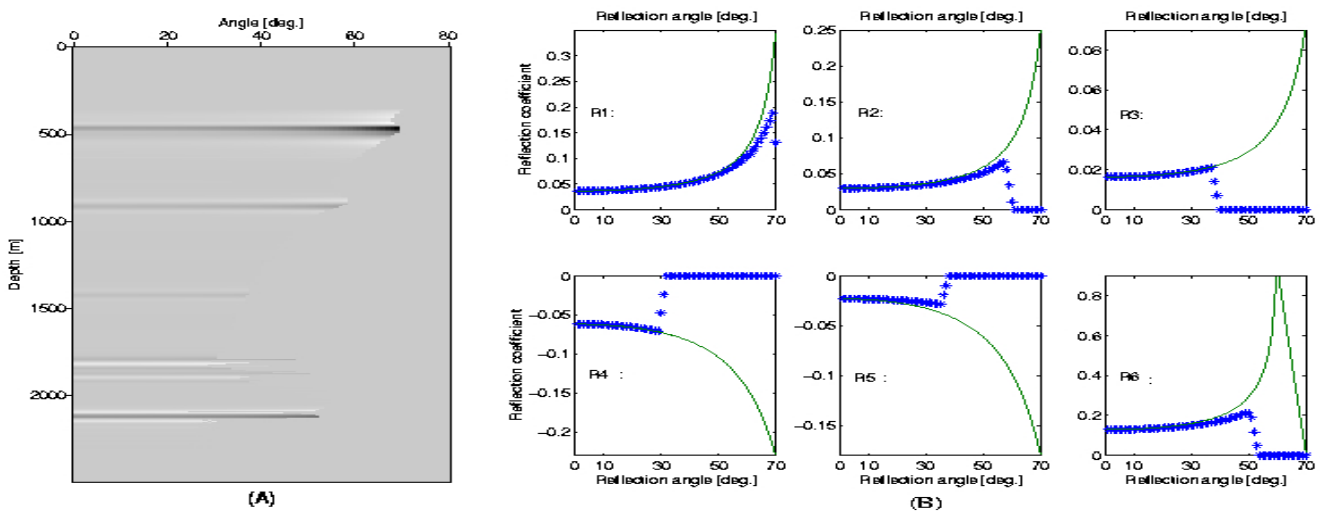


Figure 2: Migrated CIG of the synthetic data at $x = 3600$ meters (A). The corresponding picked AVA (R1 - R6) curves for six layers (B). Star line represents picked AVA, and solid line indicates the analytic curve.

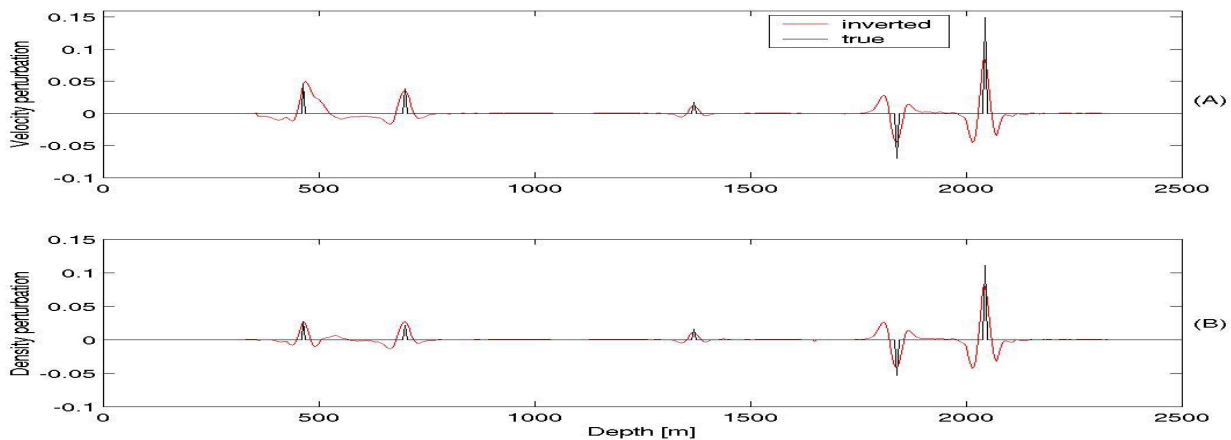


Figure 3: The comparison between inverted and true velocity (A), density (B) perturbation at $x = 2750$ meters.